


Article

Optimal Scheduling of Integrated Energy Systems with Combined Heat and Power Generation, Photovoltaic and Energy Storage Considering Battery Lifetime Loss

Yongli Wang ^{1,*}, Haiyang Yu ¹ , Mingyue Yong ², Yujing Huang ¹, Fuli Zhang ¹ and Xiaohai Wang ¹

¹ School of Economics and Management, North China Electric Power University, Changping District, Beijing 102206, China; HaiyangYU@ncepu.edu.cn (H.Y.); yujinghuang@ncepu.edu.cn (Y.H.); zhangfuli_work@163.com (F.Z.); xiaohaiwang@ncepu.edu.cn (X.W.)

² State Grid Beijing Electric Power Company, Xicheng District, Beijing 100031, China; yong_ming_yue@sina.cn

* Correspondence: wyl_2001_ren@163.com; Tel.: +86-135-8158-0878

Received: 3 June 2018; Accepted: 23 June 2018; Published: 27 June 2018



Abstract: Integrated energy systems (IESs) are considered a trending solution for the energy crisis and environmental problems. However, the diversity of energy sources and the complexity of the IES have brought challenges to the economic operation of IESs. Aiming at achieving optimal scheduling of components, an IES operation optimization model including photovoltaic, combined heat and power generation system (CHP) and battery energy storage is developed in this paper. The goal of the optimization model is to minimize the operation cost under the system constraints. For the optimization process, an optimization principle is conducted, which achieves maximized utilization of photovoltaic by adjusting the controllable units such as energy storage and gas turbine, as well as taking into account the battery lifetime loss. In addition, an integrated energy system project is taken as a research case to validate the effectiveness of the model via the improved differential evolution algorithm (IDEA). The comparison between IDEA and a traditional differential evolution algorithm shows that IDEA could find the optimal solution faster, owing to the double variation differential strategy. The simulation results in three different battery states which show that the battery lifetime loss is an inevitable factor in the optimization model, and the optimized operation cost in 2016 drastically decreased compared with actual operation data.

Keywords: integrated energy system; optimal scheduling; differential evolution; life quantification

1. Introduction

With the rapid development of society and the gradual improvement of technology, the traditional energy supply pattern is facing huge challenges, as the large scale and centralized energy supply cannot march the diverse and differential energy demand [1]. In addition, the severe energy crisis and environmental pollution problems force the energy supply pattern to be more sustainable and cleaner [2]. Hence, the integrated energy system (IES) concept, which provides flexible access to a variety of power sources, has drawn wide attention and research activity [3,4]. The IES is an extension of traditional energy applications, and it is a physical concept of a hybrid energy system, via integrating renewable energy generation, energy storage and other energy technologies, which could achieve the collaborative operation of various power sources, while obtaining certain benefits [5].

The integrated energy system consists of multiple energy subsystems. On the energy supply side, IES systems mainly exploit renewable energy sources such as wind power, photovoltaic and natural

gas, and on the energy demand side, it supplies kinds of energy to users, such as heating and electricity. However, as a complex hybrid energy system, a couple of meaningful topic need to be considered integrally, firstly the inherent fluctuation of renewable energy (RE) sources has a severe influence on the overall operation of the IES, both technically and economically, as the inherent volatility and intermittency of RE leads to difficulties in the economic scheduling of IES while providing multiple load supply. The arguments are mainly about the fact that the renewable energy generation cannot be dispatched flexibly while maintaining a certain reliability. Thus it cannot be avoided that a large amount of spare capacity must be provided to ensure the system reliability, and booming techniques such as energy storage systems (ESSs) and gas turbines are widely utilized due to their characteristics of stable output as well as speedy response [6]. However, it is inevitable that the cost would increase with the addition of components in systems, which obviously impacts the overall economy of the IES.

The integrated energy system generally consists of electric, thermal and other energy subsystems. Due to the distinct characteristics and utilization scale, the difficulty of research comparing different subsystems it greatly enhanced. Gas turbines (GTs) as a rising energy hub, can convert energy from different subsystems, and are considered to be a reliable integrated energy unit, since according to the different forms of energy demand, GTs could form a combined cooling, heating and power (CCHP) generation system or a combined heating and power (CHP) generation system via installation of suitable auxiliary equipment [7]. CHP systems are broadly utilized and researched in China due to the great energy utilization efficiency and their application feature whereby the cooling load is mostly obtained by electricity [8]. The gas turbine in a CHP generation system generally operates on the power generation mode determined by the heating load, and outputs electricity and heating power at a certain ratio. Thus, GTs are deemed an important bond to coordinate operation of hybrid energy subsystems. In the CHP generation system considered in this paper, which is the sole source of heating load in the IES, the power of the GT is determined by the heating load, thus it could be concluded that the electricity power of GT as the carrier takes part in the operation optimization of the IES.

While, the specificity of the energy storage system (ESS) due to the participation on both energy demand side and energy supply side, makes it play an important role in an IES, many relevant studies have pointed out that the ESS could ensure the power balance of the system when the load fluctuates, and the power of energy storage could be dispatched from the technical and economic level in an IES. Hence, the operation cost of storage is a key factor for the economic operation, which needs to be deeply discussed. In recent years, battery energy storage systems (BESSs) have been widely used in IESs because of their outstanding advantages. The main focus in the BESS is the battery life in different energy states during the lifecycle. In [9,10] the BESS characteristics which are the main factors that affect the life of battery, such as discharge depth, discharge rate and charge or discharge times, were analyzed. An accumulated damage model was proposed, where each discharge process could cause irreversible damage to the battery life until the battery is scrap. At the same time, the release of the electricity could be calculated from the rate of discharge depth and the rate of the discharge rate, which is called the total effective throughput, and each discharge event could be converted into effective ampere hours, when the total ampere hours reaching the total effective throughput, the battery scrap. In [11,12] an optimization model of a hybrid energy system with RE and BESS, which aims at the optimal dispatch of regulated resources considering the non-negligible frequency offset and system economic benefits was addressed. In short, the output capacity of the BESS would change under different energy states, which is reflected by the ampere hours, and it is crucial to take the lifetime loss into calculation at the time of considering the operation cost of a BESS.

The optimization objectives have a significant effect on the scheduling of the IES, so different aims would lead to the diverse dispatch of each component, so studies focusing on the optimization of the IES cover many aspects, but are mainly concentrated on the improvement of multi-target energy efficiency [13,14], economic dispatch [15] and robust optimization [9]. The applied optimization objectives of the IES operation are mostly about the economic benefit, environment benefit and system independence. Reference [16] through an analysis of a typical cogeneration system, proposed

a bus bar structure relative to the composition and structure, and then designed a scheduling optimization model, establishing a 0–1 mixed integer linear programming model for the dynamic economic dispatch of the co-supplier. Reference [17] in order to solve the problem of load uncertainty and large scale access to renewable energy, on the basis of piecewise linearization of equipment efficiency curve model, proposed a dynamic optimal scheduling strategy based on model predictive control. Reference [18] through the establishment of a comprehensive regional energy system model, obtained an optimal solution, which made the regional integrated energy system supplied by the CHP system effectively decoupled from the thermoelectric operation constraints through the energy storage equipment, thereby exerting its economic advantages and improving the energy utilization efficiency. Reference [19] focused on the optimal scheduling strategy of a CCHP energy system from the two aspects of economic optimization goal and a stochastic approach, solving the system optimization model and emphasizing the extensive application of intelligent algorithms in the field of optimal dispatch.

In addition, the optimization methodology has a great influence on the operation results, and its resolution process generally seems as a nonlinear constraint problem. The choice of model design [20], robust design [21] and optimization algorithm [22], all seem to have quite an effect on the efficiency of the solution during the resolution process. A mixed-integer linear programming model is built in [23], that could get the optimal design of hybrid energy generation systems with multiple loads, and some additional equations about the energy flow are included in the model to guarantee the effectiveness of the optimization. Besides, a robust design approach for poly generation systems is conducted in [24], which aims to obtain the proper sizing and operation method of a hybrid energy system with a CHP generation system, whereby the robustness of the CHP configuration results is developed through Pareto solutions. Evolutionary algorithms are widely used to solve such optimization problems. A comprehensive review of the various approaches contributing to the characterization, evaluation and optimization of these systems is presented in [25]. An evaluation and comparison among adequate optimization algorithms utilized in hybrid systems is given in [26]. An optimization economy model, including the power generation unit, heat pump, photovoltaic and storage which could meet the multiple demands of users was built in [27], where an advanced real time energy management system was proposed in order to optimize hybrid energy systems with renewable energy performance, where the object is minimizing the energy cost and carbon dioxide and pollutant emissions via use of a binary particle swarm optimization algorithm. It could be seen from the relevant reference that the application of intelligent algorithms to solve optimization problems is a common method, however the efficiency of optimization methodology is still a topic worth discussing.

Through the above research, it could be summarized that the integrated energy system is one of the trending energy supply patterns at present, so there is an urgent necessity for the exploration of optimal scheduling approaches for IES, which is an important and practical topic to be investigated. Much of work so far about the distribution part of IES has focused on the operation optimization based on different assumptions about conditions, and it has been demonstrated in a number of studies that different battery energy states will affect the power output to a certain extent, and there are not many studies that take the depreciation of the battery into consideration. To enhance the depth of research and improve the effectiveness of optimization in the distribution part, this paper proposed an optimization model of an IES equipped with photovoltaic (PV), BESS and a CHP generation system, while considering the battery lifetime loss. Due to the motivation of the economic dispatch of various components, an operation optimization model of an IES is established according to the coupling characteristics of heating and electric loads, and the corresponding optimization principle is put forward, as well as taking into account the coordinative operation of each units and maximization utilization of photovoltaic.

This paper aims to obtain the minimum operation cost of IES while considering battery lifetime loss. First the problem is outlined by taking into account the operation cost of the system units, then the optimization model is validated by the improved differential evolution algorithm in three

different energy states of the battery. In addition, a case study of an IES project which was put into operation in 2016 is analyzed in this paper. Compared with the operation data of the project, the optimized operation cost under the optimization principle in this paper could effectively decrease. The paper is structured as follows: the model of the integrated energy system is presented in Section 2. Section 3 describes the optimization model of the problem. The improved differential evolution algorithm methodology is proposed in Section 4, while the case study and conclusions are presented in Sections 5 and 6, respectively. The contributions of this paper can be summarized as follows:

1. We formulate an optimal scheduling problem of an IES to minimize the operation cost, which considers the randomness in stochastic renewable energy, multiple energy demands and depreciation cost of the battery for different lifetime losses.
2. The operation optimization model is verified in a case of an IES project including PV, CHP and BESS via the improved differential evolution algorithm, and a double variation strategy is applied in the IDEA to improve the validity of the solution.
3. The simulation results are analyzed, and based on the comparison with the general optimization method, which neglects battery lifetime loss in operation, we could achieve a satisfactory operation cost, and subsequent research could draw on the experience of the research results.

2. Model of the Integrated Energy System

The IES consists of a variety of energy inputs as well as multiple load outputs. This paper presents a typical IES consisting of photovoltaic, a CHP generation system, and a battery energy storage system, which could provide heating and electric power. The structure of the IES is shown in Figure 1.

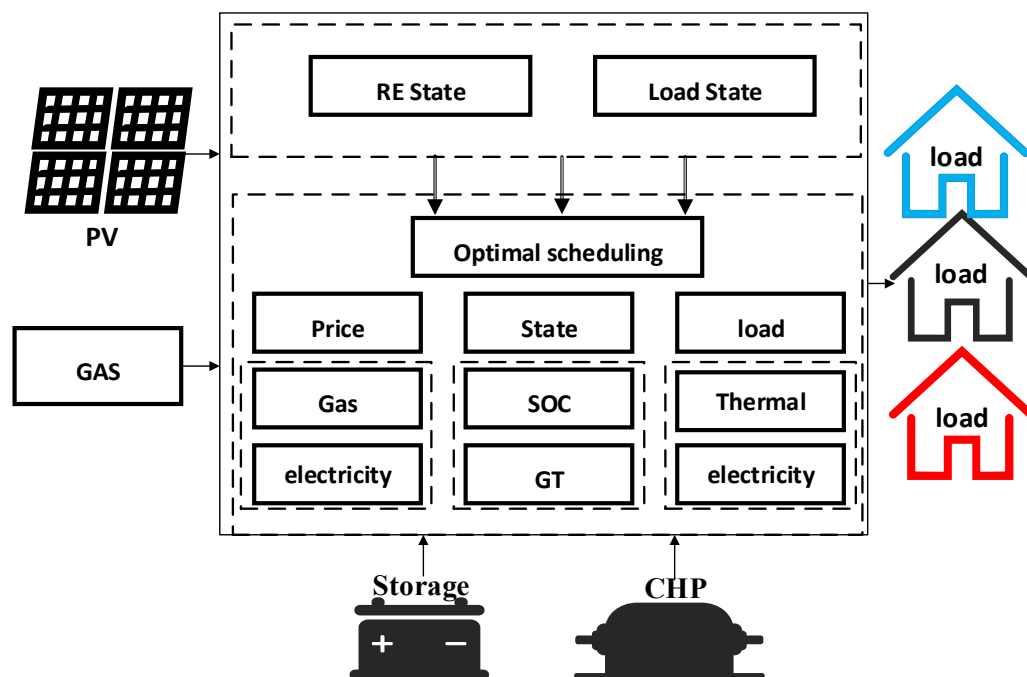


Figure 1. Schematic framework of the integrated energy system model.

This paper is focused on the optimization in the distribution side of IES. It could be seen from Figure 1 that the system includes photovoltaic energy input and natural gas input, the information input consists of the renewable energy state and multiple load state, the energy price part includes the natural gas price and electricity price, the operation state part includes the battery state reflected by the state of charge (SOC), and the gas turbine working state. According to the above parts the optimal

scheduling of IES is determined the optimization model below. The mathematical models of BESS, photovoltaic and CHP power generation are presented in [28,29].

2.1. PV Output Model

The output power of the photovoltaic (PV) depends on the photovoltaic radiation intensity and PV module temperature, which is defined as:

$$P_{pv} = f_{pv} P_{r,pv} \frac{A}{A_s} [1 + \alpha_p (T_{pv} - T_r)] \quad (1)$$

where f_{pv} is the photovoltaic output energy conversion efficiency, 0.9; $P_{r,pv}$ is the PV rated power, kW; A is the photovoltaic actual radiation intensity, W/sr; A_s is the rated radiation intensity, W/sr; α_p is the power temperature coefficient (0.47%/K), T_r is the rated PV module temperature, K; T_{pv} is the actual temperature of the PV module, K.

2.2. Energy Storage Output Model

The battery energy storage device used in this paper is a lithium-ion battery with a two state reliability mathematical model. The time sequence value of battery charging and discharging state not only depends on the exchange power of the external system, but also on the charging and discharging rate of the battery and its capacity limitation.

When the battery is in discharged state, the SOC is defined as:

$$SOC(t) = SOC(t-1) - \frac{P_{bat}(t) \cdot \Delta t}{C_{batmax} \cdot \eta_{dis}} \quad (2)$$

where $P_{bat}(t)$ is the discharge of the battery at time t , kW; η_{dis} is the discharge efficiency of the storage; SOC_{t-1} is the state of charge of the battery at time $t-1$; Δt is a simulation time interval; $C_{bat,max}$ is the nominal capacity of battery, kWh. When the battery is in charged state, the SOC is defined as:

$$SOC(t) = SOC(t-1) + \frac{P_{bat}(t) \cdot \Delta t \cdot \eta_c}{C_{bat,max}} \quad (3)$$

where η_c is the charge efficiency of the battery.

2.3. CHP Output Model

The gas turbine consists mainly of an air compressor, a gas combustion chamber, a turbine, a control system and related auxiliary equipment. Generally speaking, the gas turbine determines the type and capacity of the CHP generation system, therefore when the fuel is given, the heating power supply is a definite value, and the power generation efficiency of gas turbine is related to the output power. The amount of natural gas and the output power model are define as follows:

$$\begin{cases} Q_{GT}(t) = \frac{P_e(t) \Delta t (1 - \eta_e(t) - \eta_l)}{\eta_e(t)} \\ Q_h(t) = Q_{GT}(t) \eta_h \omega_h \end{cases} \quad (4)$$

$$V_{GT} = \frac{\sum P_e(t) \Delta t}{\eta_e(t) \times LHV_{NG}} \quad (5)$$

where $Q_{GT}(t)$, $Q_h(t)$ are the residual heat of exhaust and heating capacity at time t , kWh; $P_e(t)$ is the electric power output at time t , kW; $\eta_e(t)$ is the generator efficiency; η_l is the heat loss coefficient of gas turbine; V_{MT} is the consumption per unit time of natural gas, m³; LHV_{NG} is the low calorific value of natural gas, kWh/m³.

3. Optimization Model

3.1. Objective Function

The operation cost of an IES is generally composed of generation cost and depreciation cost, where the power generation cost mainly includes the fuel costs and maintenance costs of the generator set, which are the natural gas cost and main grid power cost in this paper, and the depreciation cost represents the costs incurred during the utilization of the equipment, where the depreciation cost of BESS is set as the object due to the great number of investment, and set ignoring the operation cost of renewable energy generation due to its small value in this paper. The target of the objective function is to minimize the operation cost of the IES through arranging the output plan of each controllable unit, and it is a non-convex problem due to the non-convex set of the units' power and the objective of purchasing the best solution. The optimization model is built below to optimize the output of each subsystem in the IES with PV, CHP generation system and BESS. In this paper, T is the time interval of simulation, which represents the step length of optimization. Since the gas turbine has a very fast response time, the T period is set as 5 min [30]. The mentioned optimization model could achieve the purpose of minimizing the operation cost of IES under the system constraints, the objective function is defined as:

$$\min C = \int_0^T (k_t P_{grid} + P_{fuel} V_{GT,t} + C_{bat,dep}) dt \quad (6)$$

where C is the operation cost of IES, yuan (i.e., 0.154 USD); P_{grid} is the main grid exchanged power, kW; when $P_{grid} > 0$, purchase power from main grid, k_t is the purchasing price at time t , yuan/kWh; on the contrary, selling the power to main grid, k_t is the selling price at time t , yuan/kWh; P_{fuel} is the natural gas price, yuan/m³; $V_{GT,t}$ is gas consumption at time t , Nm³/min; and $C_{bat,dep}$ is operation cost of battery energy storage that is the depreciation costs at per unit of time, yuan:

$$C_{bat,dep} = C_{bat} \frac{d_{act,t}}{\Gamma_{act}} = C_{bat} \frac{d_{act,t}}{\Gamma_R - \int_0^{alt} d_{act,t} dt} \quad (7)$$

$$\Gamma_R = L_R D_R C_R \quad (8)$$

where C_{bat} is the initial investment cost of BESS, yuan; alt is the total charge and discharge time that from the beginning with the energy storage, min; $d_{act,t}$ is the ampere hour in equivalent discharge current in the unit of time, Γ_R is the total throughput, Ah; L_R is the cycle number under rated power; D_R is rated discharge depth, %; C_R is rated capacity under rated discharge current, Ah.

3.2. Constraints

3.2.1. IES Operation Constraints

(1) Power balance constraint

$$P_{load} = P_{PV}(t) + P_e(t) + P_{bat}(t) + P_{grid}(t) \quad (9)$$

$$P_{thermal} = P_h(t) \quad (10)$$

where, P_{load} , $P_{thermal}$ are the total electric and thermal load of the IES at time t ; $P_{PV}(t)$, $P_{bat}(t)$ and $P_{grid}(t)$ are the electric output power of PV, battery and main grid respectively; $P_e(t)$, $P_h(t)$ are the electric and heating output power of CHP.

(2) Equipment capacity and climbing rate constraint

$$P_{i,t,min} \leq P_{i,t} \leq P_{i,t,max} \quad (11)$$

$$P_{f,t,min} \leq P_{f,t} \leq P_{f,t,max} \quad (12)$$

$P_{i,t,max}$ and $P_{i,t,min}$ are the maximum and minimum of the output power for the scheduled components such as battery and gas turbine; The $P_{f,t,max}$ and $P_{f,t,min}$ are the maximum and minimum limits of the output power of the nonscheduled power generation unit, such as PV in this paper.

When the scheduled power generation unit increases load or reduces load, there are constraints:

$$P_{i,t} - P_{i,t-1} \leq R_i^{up} \quad (13)$$

$$P_{i,t-1} - P_{i,t} \leq R_i^{down} \quad (14)$$

When non-scheduled power generation unit increases load or reduces load, there are constraints:

$$P_{f,t} - P_{f,t-1} \leq R_f^{up} \quad (15)$$

$$P_{f,t-1} - P_{f,t} \leq R_f^{down} \quad (16)$$

3.2.2. Storage Constraints

The battery energy storage system should meet the constraints of SOC and power limitation, which are expressed as:

$$SOC_{min} \leq SOC(t) \leq SOC_{max} \quad (17)$$

$$P_{ch,max} \leq P_{bat}(t) \leq P_{dis,max} \quad (18)$$

where SOC_{max} , SOC_{min} are the maximum and minimum constraints of the remaining capacity, $P_{ch,max}$, $P_{dis,max}$ are the maximum charge and discharge power.

3.2.3. Main Grid Constraint

The electric power exchange with the main grid constraints is expressed as:

$$0 < P_{grid}(t) \leq \varepsilon_{pur,max} P_{grid,max}, P_{grid} > 0 \quad (19)$$

$$0 < |P_{grid}(t)| \leq \varepsilon_{sell,max} P_{grid,max}, P_{grid} < 0 \quad (20)$$

where $P_{grid,max}$ is the maximum load exchange power with the main grid, $\varepsilon_{pur,max}$ and $\varepsilon_{sell,max}$ are the state of purchasing and selling power with main grid.

3.3. Optimization Principle

The general optimization principle of IES operation in this paper could be explained as follows: in order to achieve the purpose of operation cost savings, firstly we predict the T period electric, thermal and PV load based on the load characteristics in the $T - 1$ period. Secondly by utilizing the power of the PV and the CHP to meet the demand of electric and thermal loads, while the CHP power is determined by the heating demand. Viewed in this way, the optimization of integrated energy takes on a different meaning, where the optimization of thermal and electric energy is reflected by the optimization of electricity. One thing that could be clearly foreseen is that the PV and the CHP generation system could not balance the load demand in most situations, which could be expressed with Equation (21). At that time, the BESS would participate in the energy interaction via charging and discharging, and finally the system maintains its electric load balance through energy exchange with the main grid:

$$\begin{cases} P_{load} - P_{PV}(t) + P_e(t) > 0 \\ P_{load} - P_{PV}(t) + P_e(t) < 0 \end{cases} \quad (21)$$

For the flow of energy utilization, in order to maximize the utilization of renewable energy, the scheduling priority is usually given to renewable energy sources [31,32], such as photovoltaic power in this paper, then, for the independence of the system, priority is given to energy storage, and finally, the main grid guarantees the balance of load. For the thermal load balance, the output power of the gas turbine is determined by the thermal load, thus the electricity power of CHP is an variable determined by the thermal load value and the electricity to heat ratio.

For the energy exchange, if the battery satisfies the SOC constrain, using the power of energy storage to balance system load, and for the energy exchange with the main grid, if $P_{grid} > 0$, this means carrying out an electricity purchasing behavior, if $P_{grid} < 0$, it means carrying out an electricity selling behavior. The optimization process of a typical IES system including PV, CHP and energy storage is shown in Figure 2.

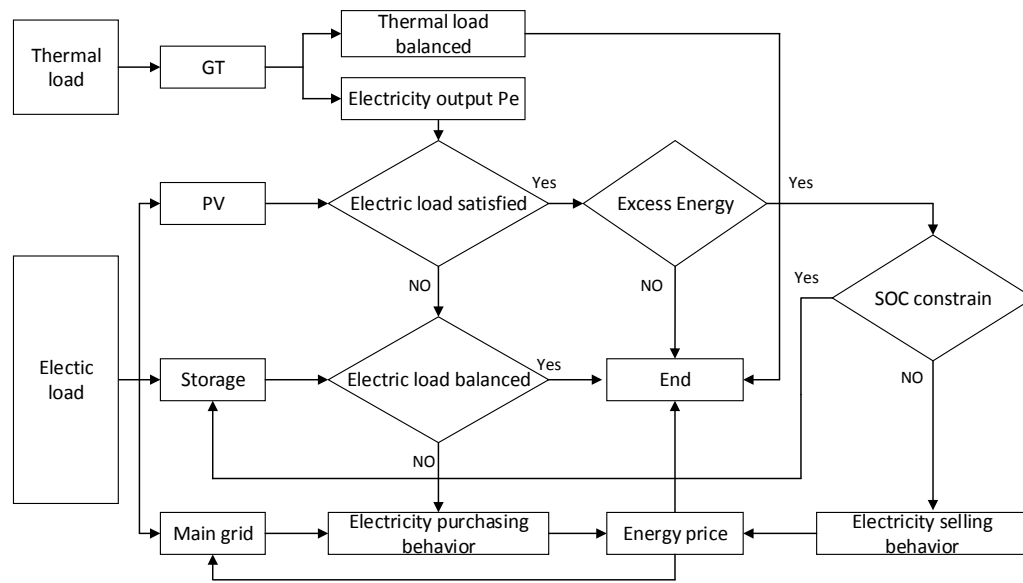


Figure 2. Optimization flowchart of a typical IES.

For the optimization process, firstly, the source of energy input is photovoltaic and natural gas, through power generation device solar panels and a CHP system providing heating and electricity power, due to the fact the power of the gas turbine is determined by the heating load, thus the electricity power is set as optimization object in this paper. Secondly, the optimization strategy is set as, when $P_{load} - P_e - P_{PV} > 0$, saving the excess energy to the battery, if the battery is full, adopting the electricity selling behavior; and when $P_{load} - P_e - P_{PV} < 0$, the battery is discharging, and if $P_{load} - P_e - P_{PV} - P_{bat} > 0$, adopting the electricity purchasing behavior, satisfying the electric load. The load of the gas turbine is determined by the heating load, and under the situation where the gas turbine cannot ensure the heating load, the outside thermal grid can support the system. Finally, the energy price is a key factor for the optimization, so we use the time of use (TOU) power price according to the electricity price situation.

4. Methodology of the Improved Differential Evolution Algorithm

4.1. Overview of the Differential Evolution Algorithm

The differential evolution algorithm (DE) is one of the optimization techniques and a kind of evolutionary computation technique, introduced by Storn and Price in 1995. The method is widely applied to solve practical optimization problems in various fields involving non-linearity, non-differentiability, multiple optima, and high dimensionality [33,34].

DE initializes a population of NP individuals and employs mutation, crossover, and selection operators at each generation to evolve its population toward the optimal direction, and DE parameters are tuned based on the strategy of adaptive parameter adjustment.

In the first step (initialization), NP individuals are initialized in the population, and each individual is called a target vector:

$$x_i = (x_{i1}^G, x_{i2}^G, \dots, x_{iD}^G), i = 1, \dots, NP \quad (22)$$

where G is the generation counter; D expresses the number of variables.

The second step is mutation, where the mutation operator is applied to generate mutant vector for each target vector. Many mutation strategies have been described in previous studies. A classical strategy is “DE/rand/1”:

$$v_i^G = x_{\Gamma_1}^G + F \times (x_{\Gamma_2}^G - x_{\Gamma_3}^G) \quad (23)$$

where F is a scale factor; Γ_1 , Γ_2 and Γ_3 are different random numbers generated from $[1, NP]$ and different from the target vector index i .

In the third step (crossover), DE employs a crossover operator to produce the trial vector u_i^G between x_i^G and v_i^G . The crossover operator performed on each component is shown as follows:

$$u_{ij}^G = \begin{cases} v_{ij}^G, & \text{if } rand \leq CR \text{ or } j = j_{rand} \\ x_{ij}^G, & \text{otherwise} \end{cases}, j = 1, 2, \dots, D \quad (24)$$

where CR is the crossover rate; j_{rand} is a randomly generated integer in $(1, D)$.

The fourth step is selection. A selection operator adopts a one-to-one competition between u_i^G and x_i^G :

$$x_i^{G+1} = \begin{cases} u_i^G, & \text{if } u_i^G \text{ is better than } x_i^G \\ x_i^G, & \text{otherwise} \end{cases} \quad (25)$$

DE repeats these three operators until a termination criterion is satisfied. Although with DE it is possible to achieve a global optimal search, it also has the disadvantage of early convergence. There are scattered random configurations at the beginning of the population, but the population density of each generation is relatively high with the development of evolution, so the exchange of information is decreasing. The evolution of individuals in the population uses the greedy selection operation which makes a simple judgment depending on the adaptability and lacks a deep rational analysis.

4.2. Improved Differential Evolution Algorithm (IDEA)

This paper introduces a double variation differential strategy to improve the population diversity, which could improve the speed and efficiency of calculation, and the local optimal solution during the iteration is avoided. Thus, due to the objective function in this paper is a non-convex problem, the improvement of the DE algorithm could fit the need of the optimization model, which is embodied in the following aspects:

(1) In the mutation operation, the improved differential evolution algorithm is used to solve the problem of population diversity loss and premature coexistence. The best (i.e., optimal individual) boot mechanism is changed to DS-best (i.e., a descending strategy based on sorting feasible solution). The improved mutation operator is shown as follows:

$$v_i^G = x_i^G + F(x_{best}^{DSG} - x_i^G) + F(x_{\Gamma_1}^G - x_{\Gamma_2}^G) \quad (26)$$

where i is random number, F is the scaling factor, which has the function of controlling the deviation vector amplification, and the value is generally in the $[0, 1]$, x_{best}^{DSG} is a DS-best individual randomly selected from $[1, rank(G)]$ intervals, G_m is the maximum number of iterations.

(2) In the process of judging population diversity, in order to avoid the problem that the algorithm falls into a local optimum with the increase of the number of iterations and the decline of population diversity, the population adaptive variance (δ^2) is introduced. When the L generation of the population average fitness variance is not improved, it is possible to determine the aggregation phenomenon of the population, so the next generation of the evolutionary population should adopt a mutation strategy to improve the diversity of the population and reduce the probability of the algorithm falling into premature convergence or local convergence. The population adaptive variance δ^2 is defined as follows:

$$\delta^2 = \frac{1}{NP} \sum_{i=1}^{NP} \left| \frac{f_i - \bar{f}}{\max\{|f_i - \bar{f}|\}} \right| \quad (27)$$

where NP is group size; f_i is the i -th individual's fitness, \bar{f} is the average fitness of the current population.

(3) By constructing a compound double mutation strategy, the deficiency of the single mutation strategy of the DE algorithm is made up. The DE/rand/1 operator with better global search performance is used as the mutation strategy 1, and the improved mutation operator DE/rand/2 is used as the mutation strategy 2. At the same time, the population diversity judgment mechanism was adopted to decide the mutation strategy used by various generations. The specific implementation of the dual mutation strategy is shown as follows:

$$v_i^G = \begin{cases} x_i^G + F(x_{best}^{DS^G} - x_i^G) + F(x_{r1}^G - x_{r2}^G) & (L \text{ reaches the default}) \\ x_i^G + F(x_{r1}^G - x_{r2}^G) & (L \text{ does not reach the default}) \end{cases} \quad (28)$$

Aiming at the IES operation optimization model constructed in this paper, the basic steps of the improved differential evolution algorithm are shown as follows:

The first step (initialization). It is assumed that there are N_i units in the IES, NP is initial population size, x_i^G is initial position.

$$NP = (x_{i,1}, x_{i,2}, x_{i,3} \dots x_{i,N_i}) \quad (29)$$

The second step: Calculate the current population fitness f_i . Enter the objective function (C) of economic operation of IES and constraints ($P_{load}, P_{thermal}, P_{i,t}, P_{f,t}, P_{grid}, SOC_t$); rank individuals from optimal to inferior according to the fitness and assign sort number.

The third step: Determine the range of the base vectors ($rank(G)$).

$$rank(G) = NP - (NP - 1) \sqrt{\frac{G}{G_m}} \quad (30)$$

The fourth step: Calculate the changes of variance in current population fitness ($\Delta\delta^2$). We could see the aggregation of the population and determine whether the algorithm is precocious by calculating $\Delta\delta^2$.

The fifth step: Calculate the population variation scaling factor $F(i)$. It is calculated by Equation (26).

The sixth step: Determine whether L reaches the default threshold and perform a dual strategy variation. If the L does not reach the default threshold, the mutation strategy 1 is executed, otherwise the mutation strategy 2 is used for mutation.

The seventh step: The mutant population is sorted and assigned according to the fitness value. Preserving the current optimal solution, if the number of iterations is not less than the maximum number of iterations G_m , then the loop ends. That is, the objective function reaches the optimal value; otherwise, the loop continues until the number of iterations is not less than the maximum number of iterations. Combined with the above analysis, the optimization process of IES operation based on the dual variation differential evolution algorithm is shown in Figure 3.

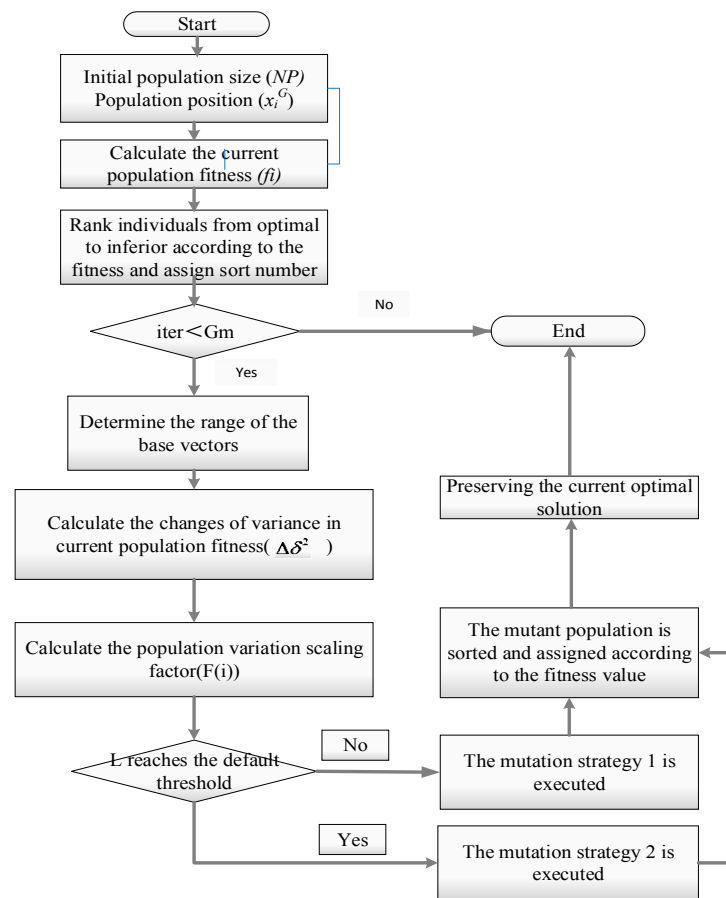


Figure 3. An improved flowchart of differential evolution algorithm.

In short, the improved differential evolution algorithm in this paper based on the double variation strategy could improve the validity of the solution, and it is suitable for solving the optimization problem in this paper. The population size and maximum variation generations need to set at first and two discriminant process would be conducted. Figure 3 shows the flowchart of IDEA.

5. Case Study

5.1. Data

In this part, an integrated energy system is modeled to verify the validation of optimization model in this paper, the IES project is selected in a industrial park which mainly contains gas turbine 1.5 MW, photovoltaic 0.4 MWp and battery energy storage system 300 kWh. The structure of the IES project is shown in Figure 4.

This integrated energy system could comprehensively regulate the electricity and thermal power in the park, at the same time, it could operate in flexible structure according to environmental conditions to meet the need of electric and thermal loads.

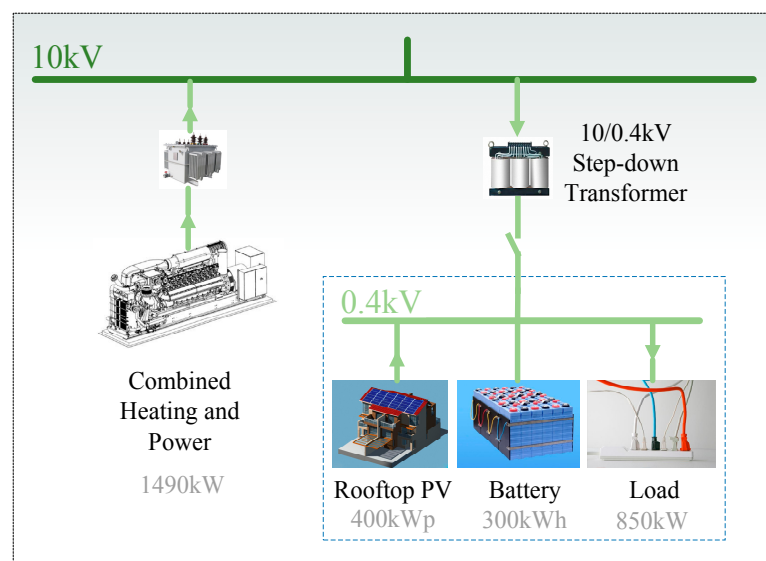


Figure 4. Structure diagram of the integrated energy system.

5.1.1. Load Data

The typical day of the system are shown as follows, the time interval of data acquisition is five minutes. The electric load in the whole year of 2016 is shown in Figure 5, and the heating load of this IES project is shown in Table 1.

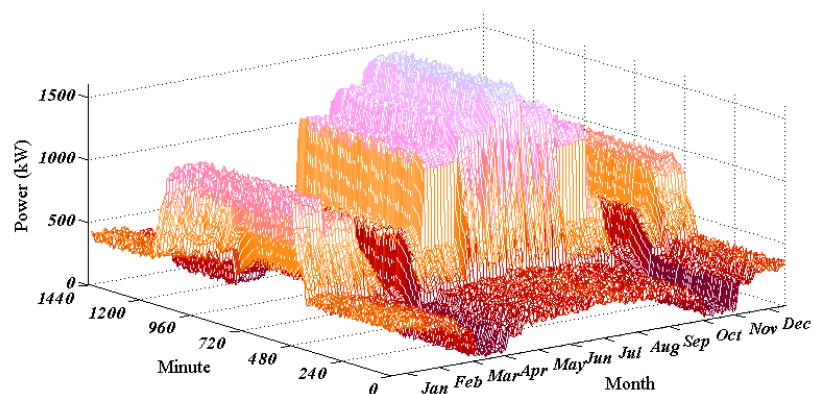


Figure 5. Electric load curve.

Table 1. Heating load statistics for IES projects.

Number	Area/m ²	Thermal Load/kW
Building 1	25,981	943
Building 2	26,996	1003
Building 3	29,850	1171
Building 4	35,735	1755
SUM	118,562	4872

5.1.2. The Energy Price Data

The price of energy has a great impact on the overall economy of the system. According to the actual situation, the price of electricity selling and the natural gas price are set as fixed prices, while the price of electricity purchasing is fluctuating in three periods, as shown in Table 2.

Table 2. Energy price (TOU).

Type	Price (¥/kWh, ¥/m ³)		
	Trough Period 0:00~6:00 18:00~24:00	Even Period 6:00~10:00 15:00~18:00	Peak Period 10:00~15:00
Electricity purchasing	0.5522	0.8185	1.2035
Electricity selling	0.65	0.65	0.65
Gas purchasing		3.16	

5.1.3. The Energy Storage Data

The total cumulative throughput of the BESS is the 1.8×10^8 Ah, the rated discharge depth is 90%, and the number of charge and discharge cycles is 2000. The main parameters of the battery are shown in Table 3.

Table 3. Main parameter value of lithium battery.

Parameter	Figure
Maximum charge discharge power/kW	65
Rated capacity/(kWh)	300
SOC operating range	0.25~0.95
SOC Overcharge protection threshold	0.9
SOC Over discharge protection threshold	0.3
Charge and discharge conversion efficiency/%	90%
Self-discharge rate/(%·s ⁻¹)	0.001
Cycle index	2000 (90% DOD)

5.1.4. The Gas Turbine Data

Table 4 lists the gas turbine parameters under the different operating conditions.

Table 4. Operation parameters of the gas turbine under different operating conditions.

Parameter	Figures under Various Operating Conditions		
Load factor/%	100	75	50
Electric power/kw	1490	1118	742
Output power/kw	1528	1146	765
Power factor	1	1	1
Voltage/V	400	399	403
Current/A	2146	1613	1064
Frequency/Hz		50	
Low calorific value/kJ/m ³		39,000	

5.2. Simulation Results

With the initial data and parameter settings given in Section 5.1, the proposed IDEA is used to obtain the optimization results based on the optimization model. To prove the effectiveness of the improvement of IDEA, the fitness curve is compared with the DE algorithm. The population size is set as $NP = 1000$, and maximum variation generations is set as $G_{\max} = 100$. The minimum value of each population variation generation is recorded, and the fitness curve and calculation time are generated iteratively, as shown in Figure 6 and Table 5.

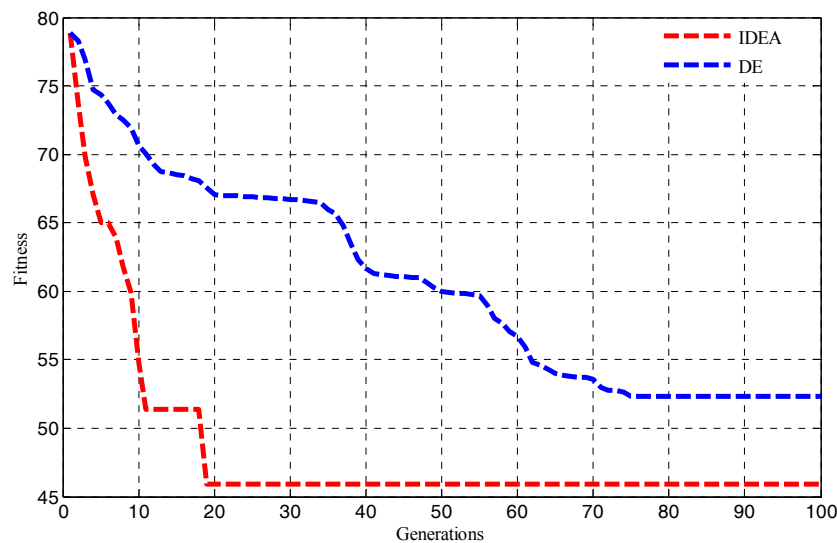


Figure 6. Adaptive curve.

Table 5. Calculation time based on DE and IDEA.

Algorithm	Optimal Generation	Calculating Time	Total CPU
IDEA	19	2.498452 s	12.016533 s
DE	78	12.702141 s	16.283614 s

As can be seen from Figure 6, compared with the traditional differential evolution algorithm, this paper uses the double mutation strategy to improve the convergence and robustness of differential evolution algorithm, it could avoid entering the local optimal solution. The optimal solution is found at the 19th time when the T period is iterated 100 times, the total calculation time is 12.0165 s, and the time for getting the optimal result is 2.4984 s. The traditional DE algorithm after 100 iterations, falls into the local optimal solution at the 78th iteration, and the total calculation time is about 16.2836 s. Therefore, it is more efficient and feasible to utilize the improved differential evolution algorithm to obtain this optimal value. In addition, for exploring the impact of the battery lifetime loss to the system operation, three cases are set based on different effective throughput of the battery, which reflects the lifetime loss of BESS:

Case 1: The cumulative throughput of BESS is 1.8×10^7 Ah, which presents a small loss of battery (i.e., 10% lifetime loss).

Case 2: The cumulative throughput of BESS is 9.0×10^7 Ah, which means some loss of battery (i.e., 50% lifetime loss).

Case 3: The cumulative throughput of BESS is 1.8×10^8 Ah, which means a major loss of battery (i.e., 100% lifetime loss).

According to the load data and parameters setting above, the optimal scheduling in the three cases is calculated through an operation optimization model. The minimum operation cost of three cases are obtained, and the scheduling plan of each unit is shown in Figure 7.

Figure 7a shows the heating and electric load at that typical day. Figure 7b–d respectively convey the scheduling plan of sources in the different BESS lifetime loss scenarios. It could be clearly seen that though we obtain the minimum operation cost in the three cases, the scheduling plans are quite different, that is an extremely thought provoking phenomenon.

Furthermore, the output power of BESS would be affected by different battery states, so it is logical that the battery with less lifetime loss would have a better performance in charging and discharging. In those three cases, the results could be directly reflected by the depth of the battery charge and the discharge depth, which are shown in Figure 8. In the first case, the battery operation cost is relatively

low due to the less energy loss, and much more charge and discharge behavior could be carried out by the BESS. In the second case, the operation cost increases, thus the curve falls slowly to 0.42 and no longer continues. In the third case, contrary to the results of the two preceding cases, the battery almost reaches its upper limit of rated cycle times, which results in a high operation cost, and the state of the battery is unchanged. Through the optimization process, the operation cost of the IES in the three cases is obtained, and the operation cost of each unit is shown in Table 6.

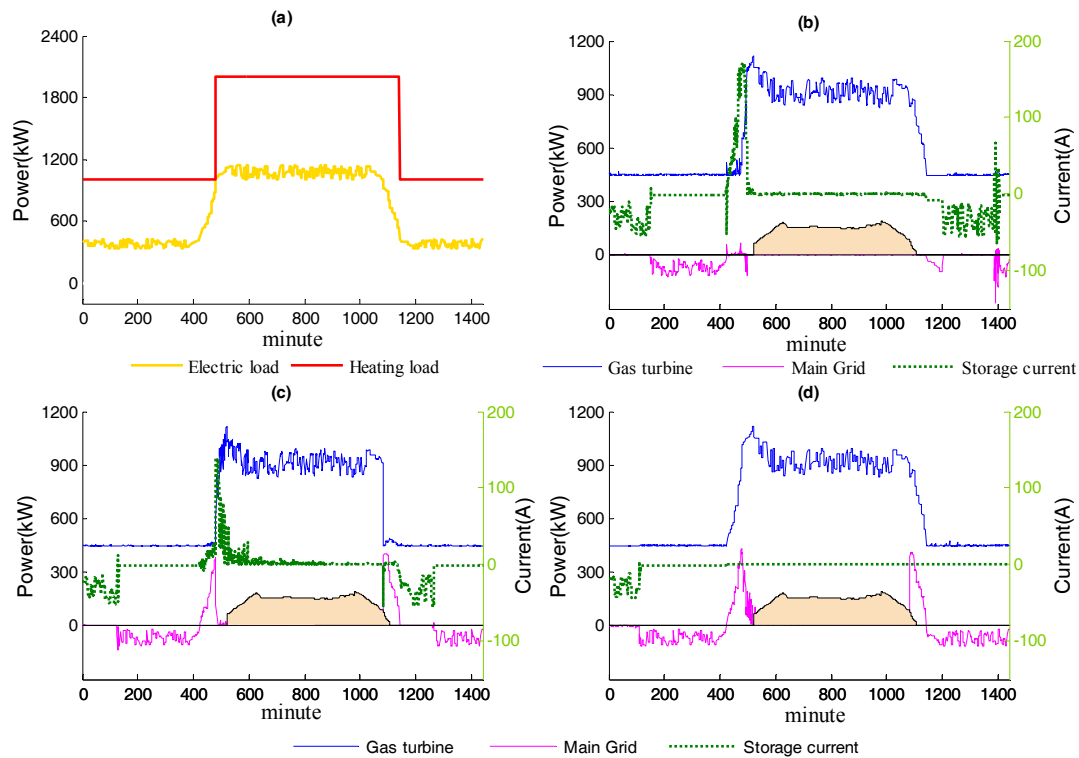


Figure 7. Optimization results in three case: (a) daily load; (b–d) optimal scheduling of Case 1, Case 2 and Case 3.

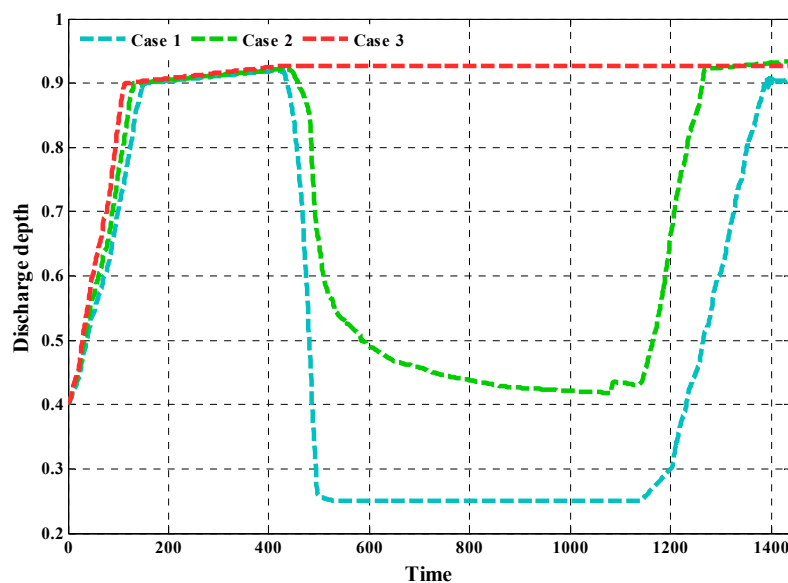


Figure 8. The depth curve of BESS in the three cases.

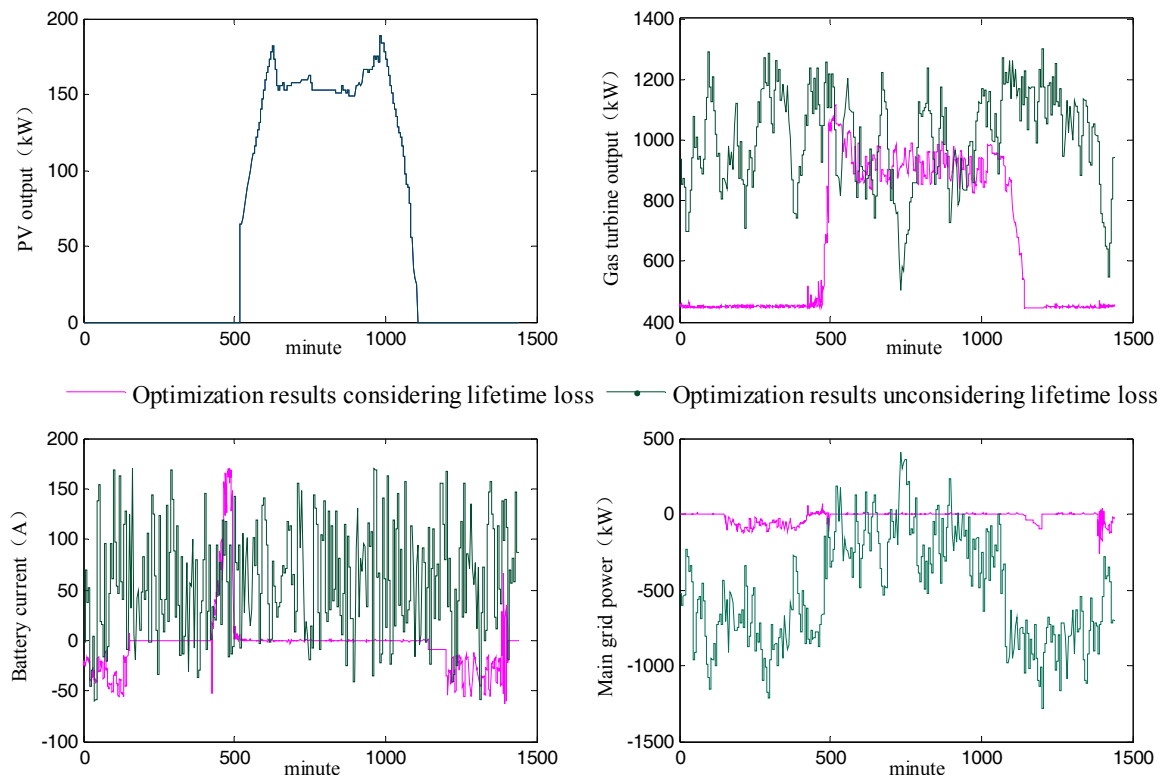
Table 6. Optimization solutions in different cases of IES.

Case	Generation Cost/Yuan			Operation Cost (Yuan)
	Main Grid	CHP	ESS	
Case 1	−840.65	11,675.86	669.25	11,504.46
Case 2	120.55	12,913.74	469.01	13,503.30
Case 3	504.71	11,491.13	181.75	12,177.59

5.3. Results Discussion

For the target of getting minimum operation cost of an IES including BESS, PV and a CHP generation system in this paper, we get the optimal scheduling in three different cases based on an operation optimization model. The improved differential evolution algorithm is used to explore the optimization results. The operation cost mainly includes the operation and depreciation cost of the units, and it could be seen from the results that fuel cost of the CHP generation system represents the largest part of the operation cost, and in Case 1 the cost of purchasing electricity is reduced due to the frequent participation of BESS, in contrast to the system where more cost of purchasing electricity from the main grid exists (Case 3).

The simulation results in this paper highlight that different energy loss states of the battery have an unavoidable influence on optimization results, which is not widely developed in the operation optimization of IES. In contrast with the optimization model in this paper, a simplified optimization model which neglects the depreciation cost of energy storage, is used to reflect the validity of the solution in this paper, and the obtained simulation results are shown in Figure 9.

**Figure 9.** Simulation results based on optimization model without considering lifetime loss of battery.

According to the comparison between the simulation results of the two optimization models, one can see the significant effect that the lifetime loss of BESS has on the optimization results. The case without considering the depreciation of BESS, which results in the more frequent charge and discharge

of the BESS, and the optimization results indicate the increase of the power cost of the gas turbine as well as the increase of exchange power with main grid, which could prove that the lifetime loss of battery is an important factor for the optimization, and the optimization model proposed in this paper could get a convincing scheduling plan for the IES.

Finally, the optimization model is applied to obtain the optimal scheduling of an IES project in whole year of 2016, and the analysis of the whole year is used to test the validation of the model. Due to the best economy of operation cost in Case 1, the cumulative throughput of BESS is set as 1.8×10^7 Ah, and the optimized results of main grid are shown in Figures 10 and 11, respectively.

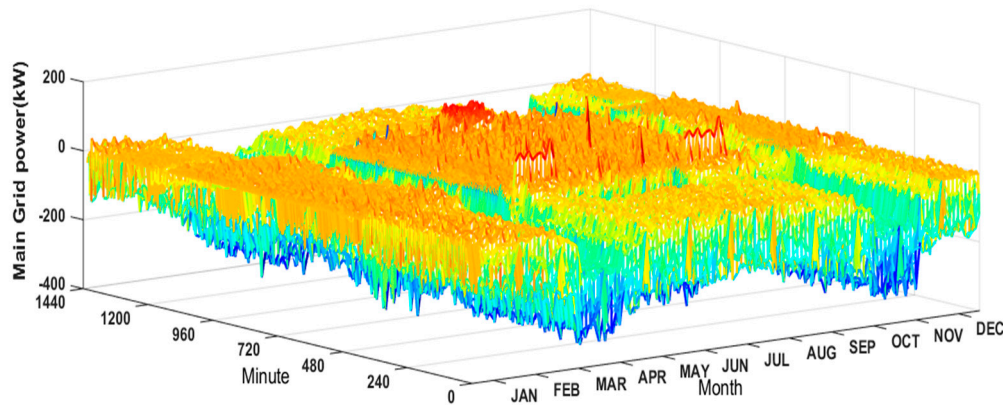


Figure 10. Optimized main grid power in 2016.

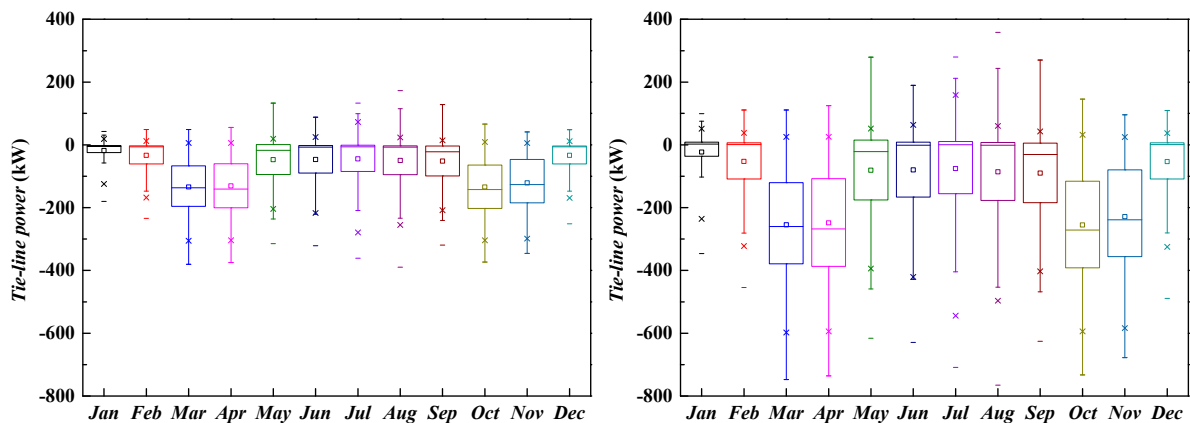


Figure 11. Monthly main grid power and actual value in 2016.

As shown in Figure 10, the optimized main grid power in 2016 of the IES is between -389.5 kW to 172.4 kW. The value of the main grid power is mostly negative, which means the system mainly conducts electricity selling behavior, which leads to a delightful independence of the IES. In addition, the optimized main grid power status and project operating cost are compared with the actual power level and actual operating cost of the project. The result is shown in Figure 11.

The left picture in Figure 11 presents the optimization result of the main grid power, and the right picture shows the actual operation state of the main grid power. The actual main grid power range is between -765.46 kW and 358.45 kW. Compared with the box line graph, it could be seen more intuitively that the purchasing power and the power in real time are respectively reduced compared to the main grid. After optimization, the absolute value of the main grid power is obviously reduced, which shows that the utilization rate of each IES source output after operation optimization is significantly improved. This is mainly reflected in the decrease of electricity selling, and at the same time guaranteeing the utilization rate as much as possible while ensuring the load demand in the

project, resulting in a reduction in the purchase of electricity. According to the purpose of getting the minimum operation cost, the operation cost of IES in 2016 is calculated through the optimization model, based on the data of 365 days, and the optimized results are shown in Figures 12 and 13.

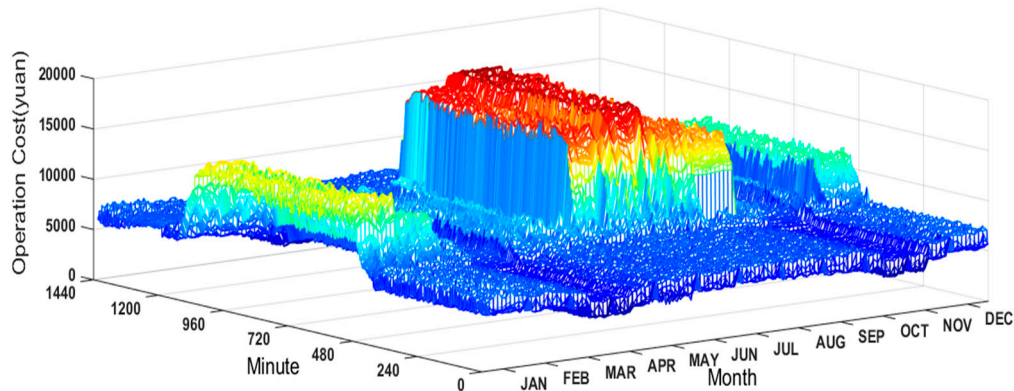


Figure 12. Optimized operation cost in 2016.

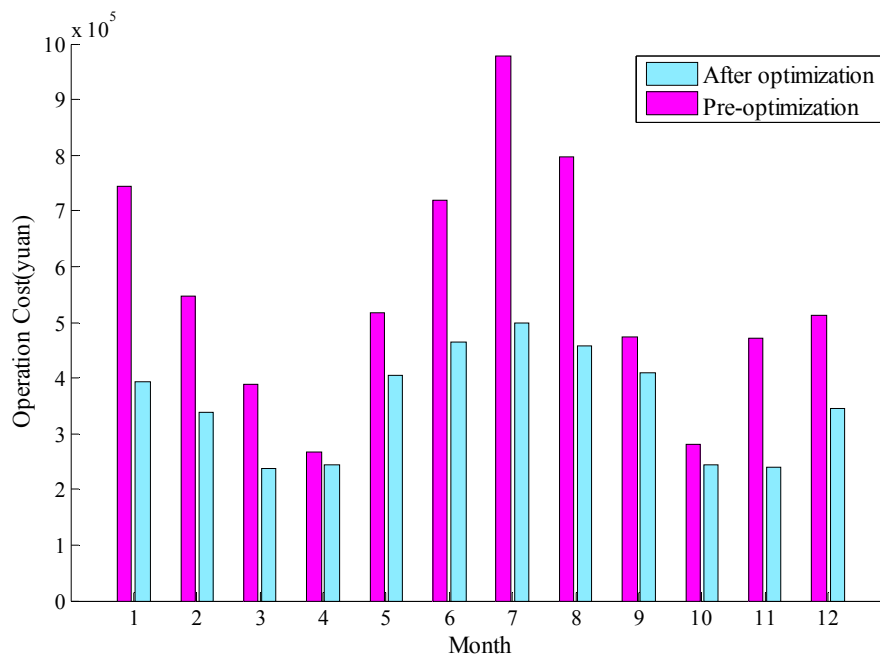


Figure 13. Monthly operation cost of IES in 2016.

As shown in Figure 12, the operation cost of the IES project in 2016 is between 3.56 to 19.95 thousand yuan. The operation costs vary in different months of 2016, and as shown in Figure 13, which reflects the total monthly actual and optimized operation cost of the project, while the actual operation cost is statistical data based on the historical records, the optimized operation cost is based on the optimization model in this paper. It could be seen that the range of the monthly operation costs before the optimization is between 0.268–0.978 million yuan, while the range of the optimized results is between 0.238–0.499 million yuan. We can come to the conclusion that the operation cost is greatly reduced by the optimization model proposed in this paper, which is especially obvious in the peak of the heating load period, where the monthly operation costs are reduced by 0.479 million yuan.

6. Conclusions

In this paper, an optimization model of an integrated energy system consisting of photovoltaic, CHP and BESS is built, which aims to get the minimum operation cost while considering the lifetime loss of battery life. It is validated in three different cases via the improved differential evolution algorithm. Our work has been presented and applied into an industrial park as a case study. The innovations and conclusions of work above could be concluded as follows:

- (1) The optimization model of IES is established considering the battery lifetime loss. Through the simulation results of three different cases, we could find the lifetime loss of battery has a great influence to the optimization results, which should not be ignored in the relevant research. We believe this solution would provide practical help to following exploration.
- (2) For the optimization searching, a double variation differential strategy is adopted to improve the population diversity, which improves the convergence speed and diversity of population. The IDEA has the characteristics of high solution speed and high accuracy compared with the traditional DE algorithm, the optimal result could be obtained by iterating the 19th generation under the setting of 100 generations.
- (3) This paper provides a more economic scheduling for IES operation, the operation optimization model proposed in this paper could effectively reduce the operation cost, and could be applied in other integrated energy systems which have a similar energy structures.

Future work will mainly cover the enrichment of IES system, such as the participation of thermal storage, the energy coupling with cooling load and the price fluctuation of natural gas. The above scenarios and constraints will be taken into consideration in the following study.

Author Contributions: F.Z. and X.W. conceived and designed the experiments; Y.H. performed the experiments; M.Y. performed the experiments; H.Y. wrote the paper; Y.W. contributed research guidance.

Funding: This work is Supported by the 111 Project (B18021) and the Fundamental Research Funds for the Central Universities (2018ZD13).

Conflicts of Interest: The authors declare no conflict of interest.

Nomenclature

P_{grid}	the main grid exchange power, kW
p_{fuel}	the gas price, ¥/m ³
V	gas consumption per unit time, Nm ³
$C_{bat,dep}$	energy storage charging or discharging depreciation costs in unit time, ¥/kWh
$C_{el,dep}$	other equipment depreciation costs per unit time
Γ_R	the total throughput
L_R	the cycle number of stored energy under rated discharge depth and rated discharge current
D_R	rated discharge depth
C_R	rated capacity under rated discharge current, Ah
D_A	the actual depth of discharge
$d_{act,t}$	the actual discharge current ampere hours in the unit of time, Ah
C_A	actual capacity, Ah
C_{bat}	the initial investment cost of energy storage, Ah
alt	the total charge discharge time from the beginning with the energy storage
q	the number of nonscheduled power generation units
P_{it}	the power output of the nonscheduled power generation unit at time t , kW
$P_{i,t,max}$	the upper bound of the active power output, kW
$P_{i,t,min}$	the lower bound of the active power output, kW
σ	the rate of self-discharged in the unit time
$\eta_{c\&dis}$	the battery charging and discharging efficiency
SOC_t	the state of charge at t time

References

1. Wang, Y. The analysis of the impacts of energy consumption on environment and public health in China. *Energy* **2010**, *35*, 4473–4479. [\[CrossRef\]](#)
2. Yüksel, I. Energy production and sustainable energy policies in Turkey. *Renew. Energy* **2010**, *35*, 1469–1476. [\[CrossRef\]](#)
3. Han, L.; Wang, F.; Tian, C. Economic Evaluation of Actively Consuming Wind Power for an Integrated Energy System Based on Game Theory. *Energies* **2018**, *11*, 1476. [\[CrossRef\]](#)
4. Ahmad, A.; Khan, A.; Javaid, N.; Hussain, H.M.; Abdul, W.; Almogren, A.; Alamri, A.; Niaz, I.A. An Optimized Home Energy Management System with Integrated Renewable Energy and Storage Resources. *Energies* **2017**, *10*, 549. [\[CrossRef\]](#)
5. Dawoud, S.M.; Lin, X.; Okba, M.I. Optimal placement of different types of RDGs based on maximization of microgrid loadability. *J. Clean. Prod.* **2017**, *168*, 63–73. [\[CrossRef\]](#)
6. Li, G.; Wang, R.; Zhang, T.; Ming, M.; Sciubba, E. Multi-Objective Optimal Design of Renewable Energy Integrated CCHP System Using PICEA-g. *Energies* **2018**, *11*, 743.
7. Liu, Y.; Gao, S.; Zhao, X.; Zhang, C.; Zhang, N. Coordinated Operation and Control of Combined Electricity and Natural Gas Systems with Thermal Storage. *Energies* **2017**, *10*, 917. [\[CrossRef\]](#)
8. Mago, P.J.; Fumo, N.; Chamra, L.M. Performance analysis of CCHP and CHP systems operating following the thermal and electric load. *Int. J. Energy Res.* **2009**, *33*, 852–864. [\[CrossRef\]](#)
9. Wang, L.; Li, Q.; Ding, R.; Sun, M.; Wang, G. Integrated scheduling of energy supply and demand in microgrids under uncertainty: A robust multi-objective optimization approach. *Energy* **2017**, *130*, 1–14. [\[CrossRef\]](#)
10. Choudhury, S.; Bhowmik, P.; Rout, P.K. Economic Load Sharing in a D-STATCOM Integrated Islanded Microgrid based on Fuzzy Logic and Seeker Optimization Approach. *Sustain. Cities Soc.* **2017**, *37*, 57–69. [\[CrossRef\]](#)
11. Hu, Y.; Li, Y.; Xu, M.; Zhou, L.; Cui, M. A Chance-Constrained Economic Dispatch Model in Wind-Thermal-Energy Storage System. *Energies* **2017**, *10*, 326. [\[CrossRef\]](#)
12. Ma, H.; Wang, B.; Gao, W.; Liu, D.; Sun, Y.; Liu, Z. Optimal Scheduling of an Regional Integrated Energy System with Energy Storage Systems for Service Regulation. *Energies* **2018**, *11*, 195. [\[CrossRef\]](#)
13. Chen, Y.; Wang, Y.; Ma, J.; Sciubba, E. Multi-Objective Optimal Energy Management for the Integrated Electrical and Natural Gas Network with Combined Cooling, Heat and Power Plants. *Energies* **2018**, *11*, 734. [\[CrossRef\]](#)
14. Dawoud, S.M.; Lin, X.; Okba, M.I. Hybrid renewable microgrid optimization techniques: A review. *Renew. Sustain. Energy Rev.* **2018**, *82*, 2039–2052. [\[CrossRef\]](#)
15. Jin, X.; Mu, Y.; Jia, H.; Wu, J.; Jiang, T.; Yu, X. Dynamic economic dispatch of a hybrid energy microgrid considering building based virtual energy storage system. *Appl. Energy* **2016**, *194*, 386–398. [\[CrossRef\]](#)
16. Wang, C.; Hong, B.; Guo, L.; Zhang, D.; Liu, W. A General Modeling Method for Optimal Dispatch of Combined Cooling, Heating and Power Microgrid. *J. China Electr. Eng.* **2013**, *33*, 26–33.
17. Wu, M.; Luo, Z.; Ji, Y.; Gu, W.; Li, Y.; Kou, L. Optimal Dynamic Dispatch for Combined Cooling, Heating and Power Microgrid Based on Model Predictive Control. *J. China Electr. Eng.* **2017**, *33*, 23–30.
18. Liu, D.; Ma, H.; Wang, B.; Gao, W.; Wang, J.; Yan, B. Operation Optimization of Regional Integrated Energy System with CCHP and Energy Storage System. *Autom. Electr. Power Syst.* **2017**, *41*, 33–40.
19. Zhou, X.; Yu, Z.; Ai, Q.; Zeng, S. Review of optimal dispatch strategy of microgrid with CCHP system. *Electr. Power Autom. Equip.* **2017**, *37*, 26–33.
20. Zhang, D.; Evangelisti, S.; Lettieri, P.; Papageorgiou, L.G. Optimal Design of CHP Based Microgrids: Multiobjective Optimisation and Life Cycle Assessment. *Energy* **2015**, *85*, 181–193. [\[CrossRef\]](#)
21. Gimelli, A.; Muccillo, M.; Sannino, R. Optimal Design of Modular Cogeneration Plants for Hospital Facilities and Robustness Evaluation of the Results. *Energy Convers. Manag.* **2017**, *134*, 20–31. [\[CrossRef\]](#)
22. Calise, F.; Capuano, D.; Vanoli, L. Dynamic Simulation and Exergo-Economic Optimization of a Hybrid Solar–Geothermal Cogeneration Plant. *Energies* **2015**, *8*, 2606–2646. [\[CrossRef\]](#)
23. Mehleri, E.D.; Sarimveis, H.; Markatos, N.C.; Papageorgiou, L.G. A Mathematical Programming Approach for Optimal Design of Distributed Energy Systems at the Neighbourhood Level. *Energy* **2012**, *44*, 96–104. [\[CrossRef\]](#)

24. Gimelli, A.; Muccillo, M. The Key Role of the Vector Optimization Algorithm and Robust Design Approach for the Design of Polygeneration Systems. *Energies* **2018**, *11*, 821. [[CrossRef](#)]
25. Ceseña, E.A.M.; Good, N.; Syrri, A.L.; Mancarella, P. Techno-Economic and Business Case Assessment of Multi-Energy Microgrids with Co-Optimization of Energy, Reserve and Reliability Services. *Appl. Energy* **2018**, *210*, 896–913. [[CrossRef](#)]
26. Chicco, G.; Mancarella, P. Distributed multi-generation: A comprehensive view. *Renew. Sustain. Energy Rev.* **2009**, *13*, 535–551. [[CrossRef](#)]
27. Lorestani, A.; Ardehali, M.M. Optimization of autonomous combined heat and power system including PVT, WT, storages, and electric heat utilizing novel evolutionary particle swarm optimization algorithm. *Renew. Energy* **2018**, *119*, 490–503. [[CrossRef](#)]
28. Wang, C.; Hong, B.; Guo, L. Dispatch Strategies of PV-Battery Microgrid in Different Scenarios. *Power Syst. Technol.* **2013**, *37*, 1775–1782.
29. Wang, F.; Zhou, L.; Wang, B.; Wang, Z.; Shafie-Khah, M.; Catalão, J.P. Modified Chaos Particle Swarm Optimization-Based Optimized Operation Model for Stand-Alone CCHP Microgrid. *Appl. Sci.* **2017**, *7*, 754. [[CrossRef](#)]
30. Wang, Y.; Huang, Y.; Wang, Y.; Li, F.; Zhang, Y.; Tian, C. Operation Optimization in a Smart Micro-Grid in the Presence of Distributed Generation and Demand Response. *Sustainability* **2018**, *10*, 847. [[CrossRef](#)]
31. Huang, Z.; Yu, H.; Chu, X.; Peng, Z. Energetic and Exergetic Analysis of Integrated Energy System Based on Parametric Method. *Energy Convers. Manag.* **2017**, *150*, 588–598. [[CrossRef](#)]
32. Zhou, Y.; Wei, Z.; Sun, G.; Cheung, K.W.; Zang, H.; Chen, S. A Robust Optimization Approach for Integrated Community Energy System in Energy and Ancillary Service Markets. *Energy* **2018**, *148*, 1–15. [[CrossRef](#)]
33. Wu, L.; Wang, Y.; Zhou, S.; Tan, W. Design of PID controller with incomplete derivation based on differential evolution algorithm. *J. Syst. Eng. Electron.* **2008**, *19*, 578–583.
34. Wang, C.; Fang, Y.; Sheng, G. Multi-objective Optimization of a Parallel Ankle Rehabilitation Robot Using Modified Differential Evolution Algorithm. *Chin. J. Mech. Eng.* **2015**, *28*, 702–715. [[CrossRef](#)]



© 2018 by the authors. Licensee MDPI, Basel, Switzerland. This article is an open access article distributed under the terms and conditions of the Creative Commons Attribution (CC BY) license (<http://creativecommons.org/licenses/by/4.0/>).